OPEN ACCESS

Single spin universal Boolean logic gate

New Journal of Physics
The open-access journal for physics

Single spin universal Boolean logic gate

H Agarwal[1], **S Pramanik and S Bandyopadhyay**[2]
Department of Electrical and Computer Engineering,
Virginia Commonwealth University, Richmond, VA 23284, USA
E-mail: sbandy@vcu.edu

New Journal of Physics **10** (2008) 015001 (15pp)
Received 11 July 2007
Published 23 January 2008
Online at http://www.njp.org/
doi:10.1088/1367-2630/10/1/015001

Abstract. Recent advances in manipulating single electron spins in quantum dots have brought us close to the realization of classical logic gates, where binary bits are encoded in spin polarizations of single electrons. Here, we show that a linear array of three quantum dots, each containing a single spin polarized electron, and with nearest neighbor exchange coupling, acts as a NAND gate. The energy dissipated during switching this gate is the Landauer–Shannon limit of $kT\ln(1/p_i)$ ($T =$ ambient temperature and $p_i =$ intrinsic gate error probability). With present day technology, $p_i = 10^{-9}$ is achievable above 1 K temperature. Even with this small intrinsic error probability, the energy dissipated during switching is only $\sim 21kT$, while today's nanoscale transistors dissipate about 40 000–50 000kT when they switch.

Contents

[1] Undergraduate summer intern visiting from Banaras Hindu University, Institute of Technology, Varanasi, India.
[2] Author to whom any correspondence should be addressed.

1. Introduction

The primary threat to progressive downscaling of electronic devices in accordance with the celebrated Moore's law [1] is the excessive energy dissipation that takes place when a device switches between logic levels. If electronic devices continue to shrink without reducing energy dissipation, thermal management will ultimately fail resulting in chip meltdown. Conventional devices have a fundamental drawback in this regard since they encode information in charge (or voltage/current levels determined by charge). Charge is a scalar quantity that has only a magnitude. Therefore, binary logic bits 0 and 1 must be demarcated by a difference in the magnitude of the charge stored in the device. Switching between logic bits would then mandate changing this magnitude, which invariably involves current flow and associated power dissipation of I^2R ($I =$ current and $R =$ resistance in the path of the current).

Spin, on the other hand, is a pseudo vector that has both a magnitude and a polarization. The polarization can be made *bistable* by placing the electron in a dc magnetic field, so that only two polarizations—parallel and anti-parallel to the field—are stable. They can encode the bits 0 and 1. Switching between them requires simply flipping the spin without physically moving the charge in space and causing a current flow. This can reduce energy dissipation significantly.

In this paper, we first show rigorously how a universal Boolean logic gate (the NAND gate) can be realized based on this idea. Although the basic idea was proposed many years ago [2], this is the first quantum mechanical calculation establishing the gate's *truth table*. Next, we present an estimate of the energy dissipated during switching. The energy dissipated in switching this gate is found to be the minimum allowed by the laws of thermodynamics, namely the Landauer–Shannon limit [3].

2. A single spin Boolean NAND gate

Consider a linear array of three single electron containing quantum dots shown in figure 1. The quantum mechanical wavefunctions of electrons in nearest-neighbor dots overlap in space causing exchange coupling between them. A weak global magnetic field makes the spin polarization in each dot bistable, because the polarization can be either parallel or anti-parallel to the global field. These two stable polarizations encode the classical binary bits 1 and 0, respectively.

The two peripheral dots A and C host the two input bits and the central dot B hosts the output bit. Input data are provided by orienting the spins in A and C in the desired directions (parallel or anti-parallel to the global magnetic field) with local magnetic fields generated by inductors, as in magnetic random access memory (MRAM) chips. These inductors are placed in the vicinity of the input dots (or wrapped around them). We will show that when the system relaxes to the ground state, the output spin polarization in dot B always conforms to the NAND function of the inputs according to the truth table (table 1).

The output can be read with a variety of techniques that are capable of single spin detection [4]–[6].

If the charging energy (intradot Coulomb repulsion) within each dot is sufficiently strong, then at half-filling (1 electron per dot), the three-spin array in figure 1 can be described by the Heisenberg Hamiltonian [7, 8].

$$H_{\text{Heisenberg}} = \sum_{\langle ij\rangle} J_{ij}^{\parallel}\sigma_{zi}\sigma_{zj} + \sum_{\langle ij\rangle} J_{ij}^{\perp}\left(\sigma_{xi}\sigma_{xj} + \sigma_{yi}\sigma_{yj}\right) + \sum_{\text{input dots}} \sigma_{zi}h_{zi}^{\text{inputs}} + \sum_{i}\sigma_{zi}h_{zi}^{\text{global}},$$

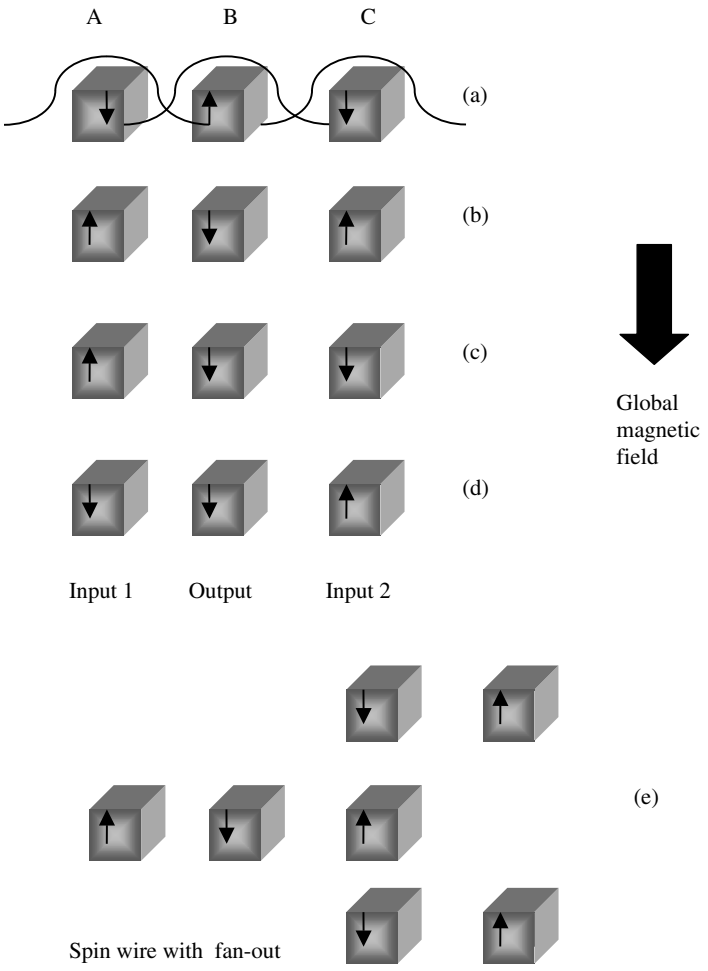

Figure 1. A single spin NAND gate: an array of three spin polarized single electrons, each housed in a quantum dot, realizes the NAND gate when the entire array is placed in a static magnetic field and allowed to relax to the thermodynamic ground state. Wavefunctions of nearest-neighbor electrons overlap (see row (a)) resulting in nearest-neighbor exchange coupling. The two peripheral spins A and C are input bits and the central spin B is the output bit. Downspin polarization (parallel to the static magnetic field) corresponds to logic bit 1 and upspin (anti-parallel to the magnetic field) to logic bit 0. When the spin polarizations in dots A and C are aligned externally to conform to the desired input bits, and the system is allowed to relax to the ground state, the spin polarization in dot B always corresponds to the NAND function of the inputs. Shown in panels (a)–(d) are the spin configurations in all three dots corresponding to the four possible input combinations of a primitive NAND gate. Panel (e) shows a 'spin wire' (with fan out) in which the spin signal is replicated in every other dot.

where the σs are Pauli spin matrices. We assume that the lowest orbital states in the quantum dots are occupied. If excitation to the higher orbital states is not accompanied by spin flip, then the higher states do not matter in the ensuing analysis, since logic bits are encoded in the

Table 1. Truth table of the NAND gate.

Input 1 (A)	Input 2 (C)	Output (B)
1	1	0
0	0	1
0	1	1
1	0	1

spin and not the orbital quantum number. Even if the rate of transition between orbital states is moderately high [9], the rate of spin flip is still very small [10], indicating that most excitations are not accompanied by spin flips. Consequently, the excited states are not important in our context. We adopt the convention that the direction of the local and the global magnetic fields is the z-direction. The last two terms in the above equation account for the Zeeman energies associated with these fields. The first two terms account for exchange interaction between nearest neighbors (the angular brackets denote summation over nearest neighbors). We will assume the isotropic case when $J_{ij}^{\perp} = J_{ij}^{\parallel} = J$, where J is the exchange energy, which is non-zero if the wavefunctions in dots i and j overlap in space.

The spins in the quantum dots are polarized in either the $+z$ or $-z$-direction, which we designate as 'upspin' ($\uparrow$) and 'downspin' ($\downarrow$) states, respectively. We will assume that the upspin state (aligned anti-parallel to the global magnetic field) encodes bit 0 and downspin state (parallel to the global field) encodes bit 1.

The three-spin basis states representing the spin configurations in the three-dot array are $|\downarrow\downarrow\downarrow\rangle$, $|\downarrow\downarrow\uparrow\rangle$, $|\downarrow\uparrow\downarrow\rangle$, $|\downarrow\uparrow\uparrow\rangle$, $|\uparrow\downarrow\downarrow\rangle$, $|\uparrow\downarrow\uparrow\rangle$, $|\uparrow\uparrow\downarrow\rangle$ and $|\uparrow\uparrow\uparrow\rangle$, where the first entry is the spin polarization in dot A, the second in dot B and the third in dot C. These eight basis functions form a complete orthonormal set. The matrix elements $\langle\phi_m|H_{\text{Heisenberg}}|\phi_n\rangle$ are given in the matrix below, where the $\phi_{m,n}$ are the three-electron basis states enumerated above.

$$\begin{pmatrix}
2J-h_A-h_C-3Z & 0 & 0 & 0 & 0 & 0 & 0 & 0 \\
0 & -h_A+h_C-Z & 2J & 0 & 0 & 0 & 0 & 0 \\
0 & 2J & -2J-h_A-h_C-Z & 0 & 2J & 0 & 0 & 0 \\
0 & 0 & 0 & -h_A+h_C+Z & 0 & 2J & 0 & 0 \\
0 & 0 & 2J & 0 & h_A-h_C-Z & 0 & 0 & 0 \\
0 & 0 & 0 & 2J & 0 & -2J+h_A+h_C+Z & 2J & 0 \\
0 & 0 & 0 & 0 & 0 & 2J & h_A-h_C+Z & 0 \\
0 & 0 & 0 & 0 & 0 & 0 & 0 & 2J+h_A+h_C+3Z
\end{pmatrix}.$$

In the above matrix, Z is one-half of the Zeeman splitting energy associated with the global magnetic field, while $2h_A$ and $2h_C$ are Zeeman splitting energies in the input dots caused by the local magnetic fields that write input data. If the local magnetic field is in the same direction as the global field and writes bit 1, then the corresponding h is positive; otherwise, it is negative. The quantity J is always positive (to guarantee that the singlet state composed of two coupled electrons has lower energy than the triplet state, as it should be).

In the appendix, we tabulate the eight eigenenergies E_n ($n = 1, \ldots, 8$) and the corresponding eigenstates

$$\begin{aligned}\psi_n = {} & c_1^n|\downarrow\downarrow\downarrow\rangle + c_2^n|\downarrow\downarrow\uparrow\rangle + c_3^n|\downarrow\uparrow\downarrow\rangle + c_4^n|\downarrow\uparrow\uparrow\rangle + c_5^n|\uparrow\downarrow\downarrow\rangle + c_6^n|\uparrow\downarrow\uparrow\rangle + c_7^n|\uparrow\uparrow\downarrow\rangle + c_8^n|\uparrow\uparrow\uparrow\rangle \\ = {} & [c_1^n, c_2^n, c_3^n, c_4^n, c_5^n, c_6^n, c_7^n, c_8^n]\end{aligned}$$

of the three-dot system obtained by evaluating the eigenvalues and eigenvectors of the above 8×8 matrix. This exercise has been carried out for four cases: $h_A = \pm h$ and $h_C = \pm h$ which correspond to the four possible input combinations, and therefore the four entries in the truth table of the NAND gate.

In the appendix, we also show that if we apply sufficiently strong local magnetic fields to orient the spins in input dots A and C to the desired directions (i.e. $|h_A| = |h_C| = h \gg J$), and allow the system to relax to the ground state, then the spin polarization in the output dot B will always represent the result of NAND Boolean logic operation on the input bits. In other words, the three-dot system *realizes a NAND gate* whenever it is in the ground state. Ground state relaxation is the central idea in some types of artificial neural networks and similar ideas are found in other contexts ([11]; the logic gate idea with quantum dashes was communicated by P Bakshi in a private communication) as well. Applying local magnetic fields exclusively to specific quantum dots that host the input bits is difficult and requires sophisticated shielding techniques and extreme spatial resolution. We visualize using spin polarized scanning tunneling microscope tips for this purpose, which can concentrate a magnetic field over a single quantum dot. A magnetic shield can be wrapped around each dot for further field containment. This is a difficult engineering challenge but not unachievable because of any fundamental physical laws.

Once the NAND gate is realized, we need only one other component to implement any arbitrary Boolean logic circuit. That element is a 'spin wire' which will ferry spin signal unidirectionally from one gate to another. A spin wire consists of a linear array of quantum dots with clock pads between them (figure 1(e)). When the clock signal at a given pad is high, the potential barrier between the two flanking dots is lowered, and their resident electrons are exchange coupled. This renders their spins anti-parallel [12]. Therefore, by sequentially clocking the barriers, we can replicate the spin bit in every other dot and transmit the spin signal along the wire unidirectionally [13].

3. Gate errors

It is the natural tendency of any physical system to relax to the ground state, which is the basis of the NAND operation. However, once a system relaxes to ground state, it need not stay there forever. If it gets out of the ground state, and it does because of noise and fluctuations [14], it will produce wrong results and cause errors in computation. We will compute this error probability next.

Consider a system which is thermodynamically coupled to its environment that allows it to relax to the ground state. Once the system has attained equilibrium with the environment, the probability of finding the system in any particular state is given by the Fermi–Dirac occupation probability. This probability is *not* unity for the ground state. If we approximate the Fermi–Dirac statistics with the Boltzmann statistics, then the ratio of the probabilities of the gate being in an excited state and the ground state is $\exp[-(E_{\text{excited}} - E_{\text{ground}})/kT]$. We can call this the error probability P_{error} associated with being in the excited state, since straying from the ground state causes an error in the result. The total error probability is the sum of P_{error} carried out over all excited states. We will call this total error probability the *intrinsic* gate error probability p_i since it accrues from the intrinsic dynamics of the gate (thermodynamics). In order to calculate p_i, we

must first find the energy differences between the ground state and the excited state. Referring to the energy eigenstates tabulated in the appendix, we find:

Case I—when inputs are [1 1]: Here $E_1 - E_{\text{ground}} \approx 4J - 2Z$ and $E_2 - E_{\text{ground}} \approx 2h + 2Z + 2J \approx 2h$, if we take into account the fact that $h \gg J, Z$. Because of the last inequality, we only have to worry about the first excited state E_1, since the second excited state E_2 is far above in energy than E_1.

Case II—inputs are [0 0]: Here, $E_1 - E_{\text{ground}} \approx 4J + 2Z$ and $E_2 - E_{\text{ground}} \approx 2h - 2Z + 2J \approx 2h$, if we again take into account the fact that $h \gg J, Z$. Therefore, the same considerations as case I apply and we only need to worry about the first excited state.

Cases III and IV—inputs are [0 1] or [1 0]: In these cases also, we need to worry only about the first excited states as long as $h \gg J, Z$, since the second excited states are far above in energy than the first excited states. Here, $E_1 - E_{\text{ground}} \approx 2Z$.

Since the total error probability is

$$p_{\text{i}} = \sum_{\text{all excited states}} P_{\text{error}} = \sum_{m=1}^{7} \text{e}^{-(E_m - E_{\text{ground}})/kT} \approx \exp[-(E_1 - E_{\text{ground}})/kT],$$

we obtain $E_1 - E_{\text{ground}} = kT\ln(1/p_{\text{i}})$. Considering the four cases above, it is obvious that we need two conditions to be fulfilled: (i) $Z = (1/2)kT\ln(1/p_{\text{i}})$ (case III or IV), and (ii) $4J - 2Z = 4J - kT\ln(1/p_{\text{i}}) = kT\ln(1/p_{\text{i}})$ (case I), which yields $J = (1/2)kT\ln(1/p_{\text{i}})$. These conditions determine the values of J and Z required to restrict the intrinsic gate error probability to not more than p_{i} at a temperature T.

There is actually a second source of gate errors caused by random, spontaneous spin flips that occur outside the computation sequence because of extraneous influences causing spin relaxation. We call the associated gate error probability the *extrinsic* error probability p_{e} since it accrues from extrinsic factors. It is easy to see that $p_{\text{e}} = 1 - \exp[-T/T_1]$ where T is the clock period and T_1 is the spontaneous spin flip time in a single quantum dot (for a single electron uncoupled with its neighbors). There are reports of $T_1 = 170\,\text{ms}$–$1\,\text{s}$ in GaAs quantum dots [10] at low temperatures and nearly 1 s in organic nanostructures [15] at even 100 K.

We emphasize that T_1 is the spin relaxation time of a single electron in an isolated quantum dot that is *uncoupled* to any of its nearest neighbors. When relaxation to ground state takes place in the logic gates during computation, each electron is exchange coupled to its nearest neighbors. This relaxation is governed by the many-body relaxation of coupled spins. The single particle spin relaxation can be orders of magnitude slower than the many body spin relaxation. This is well known in the context of the transverse relaxation time T_2 [16]. Therefore, the relaxation to ground state can occur in a time much shorter than T_1 That means that the clock frequency is not limited by $1/T_1$, but can be much higher.

In [13], we showed that the relaxation to ground state occurs when the clock signal is high and the nearest neighbors are coupled by exchange interaction. During this time, the relaxation rate is the many body rate $1/T_1^*$ which is much higher than the single particle rate $1/T_1$. When the clock signal is low, the system is in the standby state, and we would not like the spin to flip spontaneously during this time since that would cause an error. However, in the standby state, each electron is uncoupled to its neighbors and hence the spin flip rate is $1/T_1 \ll 1/T_1^*$.

The rate $1/T_1^*$ is obviously the upper limit on the clock frequency, since otherwise the relaxation to ground state will not be complete before the clock signal changes. The extrinsic error probability will be then limited by $p_e = 1 - \exp[-T_1^*/T_1] \approx T_1^*/T_1$ if $T_1^* \ll T_1$.

The intrinsic and extrinsic error probabilities are not related to each other and are independent quantities. The net error probability that error correction schemes will have to contend with is the larger of p_i and p_e. Modern error correction algorithms can handle net error probabilities as high as 3% [17].

4. Energy dissipation during switching

The maximum energy dissipated during switching the NAND gate is the largest energy difference between any two of the four ground states corresponding to the four input combinations shown in figures 1(a)–(d). By considering all the four ground state energies (see appendix), the largest energy difference between any two ground states is $2Z$ (corresponding to switching between the states in figures 1(a) and (b)), which we have just shown is $kT\ln(1/p_i)$. Therefore, the maximum energy dissipated during switching is $kT\ln(1/p_i)$. This is the well-known Landauer–Shannon limit [3].

It is interesting to note that when we switch between some of the states (e.g. between figures 1(b) and (c)), the energy dissipated is *less* than the Landauer–Shannon limit of $kT\ln(1/p_i)$. This happens because of *interactions* between the spins (internal feedback) which make all three spins act in concert as a single entity. A similar situation was addressed in [18].

In the energy calculation, we purposely ignored the energy cost of generating the local magnetic fields and the energy dissipated in the clock pads. These costs can be made arbitrarily small, certainly much smaller than $kT\ln(1/p_i)$, by adopting adiabatic schemes [19].

5. Temperature of operation

The requirement $J = Z = (1/2)kT\ln(1/p_i)$ will also determine the maximum temperature at which we can operate the logic gates if we are limited to specific values of J or Z and wish to limit p_i to a specific value. Present technological constraints limit the exchange coupling strength J to about 1 meV in semiconductor quantum dots [20] and to about 6 meV in molecules [21]. Therefore, with semiconductor quantum dot implementation, $T = 1.1\,\mathrm{K}$ if we want $p_i = 10^{-9}$ and $T = 6.5\,\mathrm{K}$ if $p_i = 0.03$, which is the maximum error probability that may be handled with the most sophisticated error correction schemes available today [17]. Conversely, if we operate at 1.1 K, then p_i can be as low as 10^{-9} in semiconductor quantum dot-based systems. Room temperature operation will require $J = 270\,\mathrm{meV}$ with $p_i = 10^{-9}$ and $J = 46\,\mathrm{meV}$ with $p_i = 0.03$. Neither value of J is achievable with semiconductor quantum dots or molecular magnets at present, which unfortunately precludes room temperature operation with present day technology. Future technological advances may make room temperature operation feasible.

If we operate at 1.1 K with $p_i = 10^{-9}$, then $Z = g\mu_B B_{\mathrm{global}} = kT\ln(1/p_i) = 1\,\mathrm{meV}$. Here, g is the g-factor of the quantum dot material and B_{global} is the magnetic flux density of the global magnetic field. We can make B_{global} small by using materials with large g-factors. If we use $InSb_{1-x}N_x$, which is predicted to have a g-factor of 900 [22], then $B_{\mathrm{global}} = 0.04\,\mathrm{T}$ if $Z = 1\,\mathrm{meV}$.

The local magnetic fields needed to write input bits in dots A and C need to be approximately 10 times larger than the global field (see appendix). Therefore, the local field strengths need not exceed 0.4 T, which should be within reach of MRAM technology [23].

Finally, one concern is that using a material with giant g-factor may adversely affect the spin flip time. But it will affect T_1 and T_1^* almost equally. Therefore, the extrinsic error probability $p_e = T_1^*/T_1$, will not change by much. If T_1^* goes down, then the maximum clock frequency $1/T_1^*$ will increase commensurately.

6. Conclusion

We have shown that a simple linear array of three spins in quantum dots, with nearest-neighbor exchange coupling, realizes the universal classical Boolean NAND gate, if placed in a global dc magnetic field and allowed to relax to the thermodynamic ground state. Recent advances in single spin electronics, allowing control over single electrons, has brought us close to the realization of such computing elements [24]–[26]. The energy dissipated during switching between states is $\sim 21kT$ with an intrinsic error probability as low as 10^{-9} which is much better than the 40 000–50 000kT dissipated in present day transistor-based gates [27]. The temperature of operation is $\sim$1 K due to present constraints in quantum dot technology. At this temperature, the energy dissipated during switching is $\sim 3 \times 10^{-22}$ J if $p_i = 10^{-9}$. This can extend Moore's law easily into the next few decades. We also point out that realization of these gates does not require phase coherence of spin, which is difficult to preserve over long times. This paradigm is completely classical unlike quantum computing; therefore, these gates are considerably easier to implement than quantum gates.

Acknowledgments

This work is supported by the US Air Force Office of Scientific Research under grant FA9550-04-1-0261 and by the US National Science Foundation under grant CCF-0726373. The conclusions in this paper are those of the authors and do not represent an endorsement by the National Science Foundation.

Appendix

We tabulate below the eight many-body eigenenergies (E_n) and the eigenstates (ψ_n) of the three-spin array for the four cases corresponding to the four input combinations shown in figures 1(a)–(d).

Case I: $\boldsymbol{h_A = h_C = h > 0}$: this is the case when the input bits are [1 1] and the situation corresponds to figure 1(a) (the first entry in the truth table of the NAND gate). The eight eigenenergies E_n and eigenstates ψ_n are shown in table A.1.

Table A.1. Eigenenergies and eigenstates when the inputs are [1 1]; $h_A = h_C = h > 0$.

Eigenenergies (E_n)	Eigenstates (ψ_n)
$-J-h-Z-\Delta_1$	$[0, 2/\beta_1, \alpha_1/(J\beta_1), 0, 2/\beta_1, 0, 0, 0]$
$2J-2h-3Z$	$[1, 0, 0, 0, 0, 0, 0, 0]$
$-J+h+Z-\Delta_2$	$[0, 0, 0, 2/\beta_3, 0, -\alpha_3/(J\beta_3), 2/\beta_3, 0]$
$-Z$	$[0, 1/\sqrt{2}, 0, 0, -1/\sqrt{2}, 0, 0, 0]$
Z	$[0, 0, 0, -1/\sqrt{2}, 0, 0, 1/\sqrt{2}, 0]$
$-J-h-Z+\Delta_1$	$[0, 2/\beta_6, \alpha_6/(J\beta_6), 0, 2/\beta_6, 0, 0, 0]$
$-J+h+Z+\Delta_2$	$[0, 0, 0, 2/\beta_7, 0, -\alpha_7/(J\beta_7), 2/\beta_7, 0]$
$2J+2h+3Z$	$[0, 0, 0, 0, 0, 0, 0, 1]$

where

$$\Delta_1 = \sqrt{(h+J)^2+8J^2},$$
$$\Delta_2 = \sqrt{(h-J)^2+8J^2},$$
$$\alpha_1 = -J-h-\Delta_1,$$
$$\alpha_3 = J-h+\Delta_2,$$
$$\alpha_6 = -J-h+\Delta_1,$$
$$\alpha_7 = J-h-\Delta_2,$$
$$\beta_n = \sqrt{(\alpha_n/J)^2+8}.$$

Note that the eigenenergies E_n depend on Z, but the eigenstates ψ_n do not. In table A.1, the eigenenergies are arranged in ascending order (i.e. the first entry is the ground state and the last entry is the highest excited state), *provided* $h \gg J$ *and* $J > Z/2$. The reason to ensure the first inequality will become clear now.

Note that the ground state wavefunction is the entangled state

$$\psi^{11}_{\text{ground}} = \frac{2}{\beta_1}|\downarrow\downarrow\uparrow\rangle + \frac{\alpha_1}{J\beta_1}|\downarrow\uparrow\downarrow\rangle + \frac{2}{\beta_1}|\uparrow\downarrow\downarrow\rangle.$$

However, when the inputs are [1 1], or [↓, ↓], we want the output to be [0], or [↑] since this is the situation shown in figure 1(a). Therefore, the *desired* ground state is the unentangled state

$$\psi^{11}_{\text{desired}} = |\downarrow\uparrow\downarrow\rangle.$$

Obviously, we can make $\psi^{11}_{\text{ground}} \approx \psi^{11}_{\text{desired}}$ if

$$\left|\frac{\alpha_1}{2J}\right| = \frac{h+J+\sqrt{(h+J)^2+8J^2}}{2J} \gg 1,$$

i.e. if $h \gg J$. In other words, the three-spin configuration in figure 1(a) will become the ground state if we make $h \gg J$. In that case, whenever we apply the inputs [1, 1] to the input dots A and

Table A.2. Eigenenergies and eigenstates when the inputs are [0 0]; $h_A = h_C = -h < 0$.

Eigenenergies	Eigenstates
$-J-h+Z-\Delta_1$	$[0, 0, 0, 2/\beta_3, 0, \alpha_3/(J\beta_3), 2/\beta_1, 0]$
$2J-2h+3Z$	$[0, 0, 0, 0, 0, 0, 0, 1]$
$-J+h-Z-\Delta_2$	$[0, 2/\beta_3 - \alpha_3/(J\beta_3), 0, 2/\beta_3, 0, 0, 0]$
$-Z$	$[0 - 1/\sqrt{2}, 0, 0, 1/\sqrt{2}, 0, 0, 0]$
Z	$[0, 0, 0, -1/\sqrt{2}, 0, 0, 1/\sqrt{2}, 0]$
$-J-h+Z+\Delta_1$	$[0, 0, 0, 2/\beta_6, 0, -\alpha_6/(J\beta_6), 2/\beta_6, 0]$
$-J+h-Z+\Delta_2$	$[0, 2/\beta_7, \alpha_7/(J\beta_7), 0, 2/\beta_7, 0, 0, 0]$
$2J+2h-3Z$	$[1, 0, 0, 0, 0, 0, 0, 0]$

C and let the system relax thermodynamically to the ground state (by emitting phonons, etc), it will reach the state in figure 1(a) where the output bit (in dot B) will be [0] and *we will have realized the first entry in the truth table of the NAND gate.*

Case II: $\boldsymbol{h_A = h_C = -h < 0}$: This is the case when the input bits are [0 0] and the situation corresponds to figure 1(b). For this case, the eigenenergies and eigenstates are obtained by replacing the quantity h in table A.1 with $-h$.

In this case, the ground state wavefunction is the entangled state

$$\psi^{00}_{\text{ground}} = \frac{2}{\beta_1}|{\downarrow\uparrow\uparrow}\rangle + \frac{\alpha_1}{J\beta_1}|{\uparrow\downarrow\uparrow}\rangle + \frac{2}{\beta_1}|{\uparrow\uparrow\downarrow}\rangle,$$

whereas the desired state shown in figure 1(b) is the unentangled state

$$\psi^{00}_{\text{desired}} = |{\uparrow\downarrow\uparrow}\rangle.$$

Once again, we can make $\psi^{00}_{\text{ground}} \approx \psi^{00}_{\text{desired}}$ if we make $|\alpha_1/2J| \gg 1$, or $h \gg J$. Then, if we apply inputs [00] to dots A and C, and let the system relax to the ground state, dot B will have output [1] corresponding to figure 1(b), and we will have realized the second entry in the truth table of the NAND gate. All we need for this to happen is $h \gg J$.

Case III: $\boldsymbol{-h_A = h_C = h > 0}$: This is the case when the input bits are [0 1] and the situation corresponds to figure 1(c). In this case, the eigenenergies and eigenstates are more complicated and given in table A.3, where

$$\theta_1 = J\left[9(h/J)^2 - 10 + 3\mathrm{i}\sqrt{3(h/J)^6 + 12(h/J)^4 + 69(h/J)^2 + 27}\right]^{1/3},$$

$$\theta_2 = -\frac{4J^2}{3\theta_1}\left[(h/J)^2 + 7/3\right],$$

$$\theta_3 = \frac{2\theta_1}{3} + \frac{3\theta_2}{2} = 2\mathrm{i}\,\mathrm{Im}\left(\frac{2\theta_1}{3}\right),$$

$$\theta_4 = \frac{2\theta_1}{3} - \frac{3\theta_2}{2} = 2\,\mathrm{Re}\left(\frac{2\theta_1}{3}\right),$$

Table A.3. Eigenenergies and eigenstates when the inputs are [0 1]; $-h_{\mathrm{A}} = h_{\mathrm{C}} = h > 0$.

Eigenenergies	Eigenstates
$-\theta_4 - 2J/3 - Z + (\sqrt{3}\mathrm{i}/2)\theta_3$	$[0, \pi_3^{(1)}/(J^2\pi_4^{(1)}), 2\pi_1^{(1)}/(J\pi_4^{(1)}), 0, 4/\pi_4^{(1)}, 0, 0, 0]$
$-\theta_4 - 2J/3 + Z + (\sqrt{3}\mathrm{i}/2)\theta_3$	$[0, 0, 0, \pi_3^{(2)}/(J^2\pi_4^{(2)}), 0, 2\pi_1^{(2)}/(J\pi_4^{(2)}), 4/\pi_4^{(2)}, 0]$
$-\theta_4 - 2J/3 - Z - (\sqrt{3}\mathrm{i}/2)\theta_3$	$[0, \pi_3^{(3)}/(J^2\pi_4^{(3)}), 2\pi_1^{(3)}/(J\pi_4^{(3)}), 0, 4/\pi_4^{(3)}, 0, 0, 0]$
$-\theta_4 - 2J/3 + Z - (\sqrt{3}\mathrm{i}/2)\theta_3$	$[0, 0, 0, \pi_3^{(4)}/(J^2\pi_4^{(4)}), 0, 2\pi_1^{(4)}/(J\pi_4^{(4)}), 4/\pi_4^{(4)}, 0]$
$2J - 3Z$	$[1, 0, 0, 0, 0, 0, 0, 0]$
$2J + 3Z$	$[0, 0, 0, 0, 0, 0, 0, 1]$
$\theta_4 - 2J/3 - Z$	$[0, \pi_3^{(7)}/(J^2\pi_4^{(7)}), 2\pi_1^{(7)}/(J\pi_4^{(7)}), 0, 4/\pi_4^{(7)}, 0, 0, 0]$
$\theta_4 - 2J/3 + Z$	$[0, 0, 0, \pi_3^{(8)}/(J^2\pi_4^{(8)}), 0, 2\pi_1^{(8)}/(J\pi_4^{(8)}), 4/\pi_4^{(8)}, 0]$

$$\pi_1^{(1)} = -\theta_4/2 - 2J/3 + 2h + (\sqrt{3}\mathrm{i}/2)\theta_3,$$
$$\pi_2^{(1)} = -\theta_4/2 - 2J/3 - Z + (\sqrt{3}\mathrm{i}/2)\theta_3,$$
$$\pi_3^{(1)} = \left[\pi_2^{(1)}\right]^2 + 2\pi_2^{(1)}(Z + J + h) + 4Jh + 2JZ - 4J^2 + Z^2 + 2hZ,$$

$$\pi_1^{(2)} = \pi_1^{(1)},$$
$$\pi_2^{(2)} = \pi_2^{(1)} + 2Z,$$
$$\pi_3^{(2)} = \left[\pi_2^{(2)}\right]^2 + 2\pi_2^{(2)}(-Z + J + h) + 4Jh - 2JZ - 4J^2 + Z^2 - 2hZ,$$

$$\pi_1^{(3)} = \pi_1^{(1)} - \sqrt{3}\mathrm{i}\theta_3,$$
$$\pi_2^{(3)} = \pi_2^{(1)} - \sqrt{3}\mathrm{i}\theta_3,$$
$$\pi_3^{(3)} = \left[\pi_2^{(3)}\right]^2 + 2\pi_2^{(3)}(Z + J + h) + 4Jh + 2JZ - 4J^2 + Z^2 + 2hZ,$$

$$\pi_1^{(4)} = \pi_1^{(2)} - \sqrt{3}\mathrm{i}\theta_3,$$
$$\pi_2^{(4)} = \pi_2^{(2)} - \sqrt{3}\mathrm{i}\theta_3,$$
$$\pi_3^{(4)} = \left[\pi_2^{(4)}\right]^2 + 2\pi_2^{(4)}(-Z + J + h) + 4Jh - 2JZ - 4J^2 + Z^2 - 2hZ,$$

$$\pi_1^{(7)} = \theta_4 - 2J/3 + 2h,$$
$$\pi_2^{(7)} = \theta_4 - 2J/3 - Z,$$
$$\pi_3^{(7)} = \left[\pi_2^{(7)}\right]^2 + 2\pi_2^{(7)}(Z + J + h) + 4Jh + 2JZ - 4J^2 + Z^2 + 2hZ,$$

$$\pi_1^{(8)} = \pi_1^{(7)},$$
$$\pi_2^{(8)} = \pi_2^{(7)} + 2Z,$$

$$\pi_3^{(8)} = \left[\pi_2^{(8)}\right]^2 + 2\pi_2^{(8)}\,(-Z + J + h) + 4Jh - 2JZ - 4J^2 + Z^2 - 2hZ,$$

$$\pi_4^{(n)} = \left[\frac{\left[\pi_3^{(n)}\right]^2}{J^4} + \frac{4\left[\pi_1^{(n)}\right]^2}{J^2} + 16\right]^{1/2}, \quad (n = 1, \ldots, 8).$$

The ground state wavefunction is given by the entangled state

$$\psi_{\text{ground}}^{01} = \frac{\pi_3^{(1)}}{J^2\pi_4^{(1)}}\,|{\downarrow\downarrow\uparrow}\rangle + \frac{2\pi_1^{(1)}}{J\pi_4^{(1)}}\,|{\downarrow\uparrow\downarrow}\rangle + \frac{4}{\pi_4^{(1)}}\,|{\uparrow\downarrow\downarrow}\rangle,$$

whereas the desired state shown in figure 1(c) is the unentangled state

$$\psi_{\text{desired}}^{01} = |{\uparrow\downarrow\downarrow}\rangle.$$

Once again, we can make $\psi_{\text{ground}}^{10} \approx \psi_{\text{desired}}^{10}$ if we make $h \gg J$. Therefore, if we apply inputs [0 1] to dots A and C and let the system relax to the ground state, dot B will have output [1] corresponding to figure 1(c), and we will have realized the third entry in the truth table of the NAND gate.

Case IV: $-\boldsymbol{h_A}=\boldsymbol{h_C}=-\boldsymbol{h}<\mathbf{0}$. This is the case when the input bits are [1 0] and the situation corresponds to figure 1(d). The eigenenergies do not change from table A.3 since they depend on h^2 and are therefore insensitive to the sign of h. However, the eigenstates are sensitive to the sign of h and change. The eight eigenstates can be found by replacing $\pi_p^{(q)}$ by $\hat{\pi}_p^{(q)}$ where,

$$\hat{\pi}_p^{(q)}(h) = \pi_p^{(q)}(-h), \quad (p = 1, \ldots, 4, q = 1, \ldots, 8).$$

The ground state wavefunction is given by the entangled state

$$\psi_{\text{ground}}^{10} = \frac{\hat{\pi}_3^{(1)}}{J^2\hat{\pi}_4^{(1)}}\,|{\downarrow\downarrow\uparrow}\rangle + \frac{2\hat{\pi}_1^{(1)}}{J\hat{\pi}_4^{(1)}}\,|{\downarrow\uparrow\downarrow}\rangle + \frac{4}{\hat{\pi}_4^{(1)}}\,|{\uparrow\downarrow\downarrow}\rangle,$$

while the desired state shown in figure 1(d) is the unentangled state

$$\psi_{\text{desired}}^{10} = |{\downarrow\downarrow\uparrow}\rangle.$$

It is easy to check that we can make $\psi_{\text{ground}}^{10} \approx \psi_{\text{desired}}^{10}$ if we make $h \gg J$. Therefore, if we apply inputs [10] to dots A and C and let the system relax to the ground state, dot B will have output [1] corresponding to figure 1(d), and we will have realized the fourth and final entry in the truth table of the NAND gate.

In conclusion, what we have shown here is that if we place a three-spin array with nearest-neighbor exchange coupling in a dc magnetic field, and align the spins in the two peripheral dots (designated as input ports) with sufficiently strong local magnetic field B_{local} such that the Zeeman splitting in the inputs dots $2h = g\mu_B B_{\text{local}}$ is much larger than $2J$, then the spin polarization in the output (central) dot will always conform to the NAND function of the two inputs, once the array relaxes to the thermodynamic ground state. This realizes a 'single-spin-NAND-gate'.

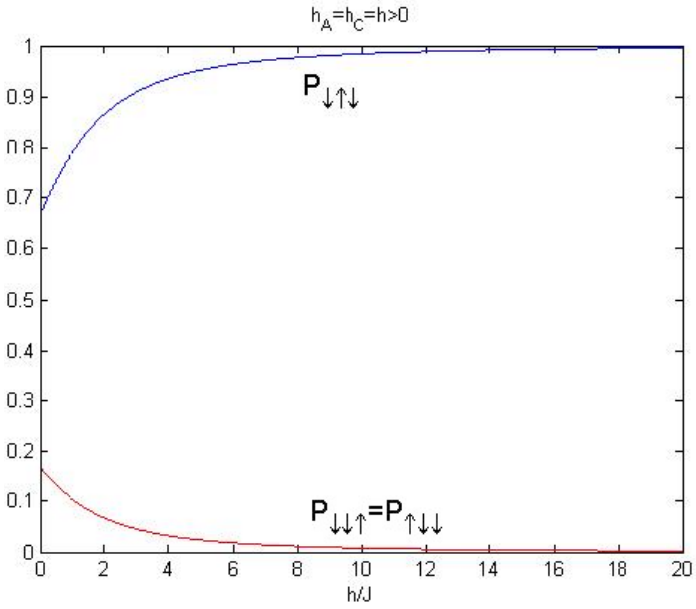

Figure A.1. Probabilities as a function of the ratio h/J when the inputs bits are [1 1].

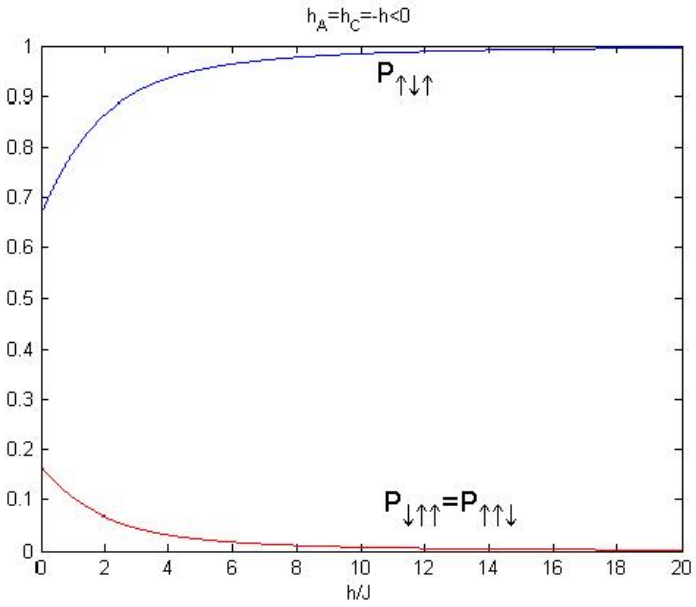

Figure A.2. Probabilities as a function of the ratio h/J when the inputs bits are [0 0].

One final issue that needs to be resolved is the following. In order for the NAND gate to work correctly, we need that $h \gg J$. How large should the ratio h/J be? Note from table A.1 that the ground state approaches the unentangled state $|\downarrow\uparrow\downarrow\rangle$ if $|\alpha_1/(J\beta_1)| \to 1$ and $|2/\beta_1| \to 0$. Let us define $P_{\downarrow\uparrow\downarrow} = |\alpha_1/(J\beta_1)|^2$ and $P_{\downarrow\downarrow\uparrow} = P_{\uparrow\downarrow\downarrow} = |2/\beta_1|^2$ since $\alpha_1/(J\beta_1)$ is the amplitude of the $|\downarrow\uparrow\downarrow\rangle$ component and $2/\beta_1$is the amplitude of the $|\downarrow\downarrow\uparrow\rangle$ or $|\uparrow\downarrow\downarrow\rangle$ components in the ground

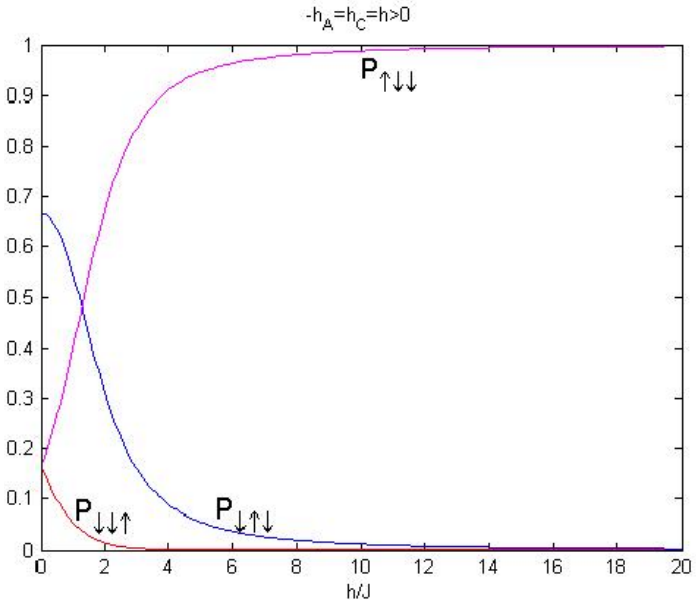

Figure A.3. Probabilities as a function of the ratio *h/J* when the inputs bits are [0 1].

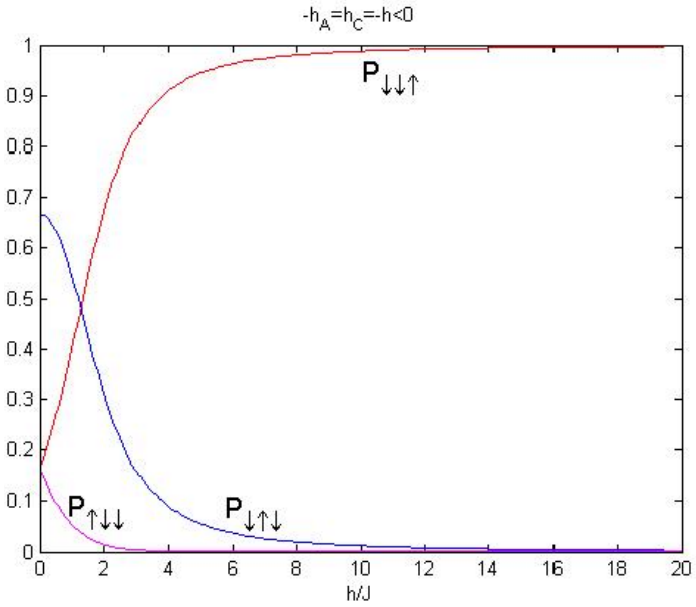

Figure A.4. Probabilities as a function of the ratio *h/J* when the inputs bits are [1 0].

state wavefunction. In figure A.1, we plot these quantities as a function of the ratio h/J. Note that $|\alpha_1/(J\beta_1)| \to 1$ and $|2/\beta_1|0$ when $h/J \geqslant 10$. Therefore, in case I, we need $h/J \geqslant 10$ to make the ground state nearly indistinguishable from the unentangled state $|\downarrow\uparrow\downarrow\rangle$.

In figures A.2–A.4, we plot the equivalent quantities for cases II, III and IV, respectively. Once again, we find that ensuring $h/J > 10$ is sufficient.

Therefore, in all cases, it is adequate to have the strengths of the local magnetic fields writing inputs bits no more than 10 times stronger than the global magnetic field. If the global magnetic flux density is 0.04 T, it is sufficient to have the local magnetic flux density 0.4 T.

References

[1] Moore G E 1965 *Electronics Magazine* (New York: McGraw Hill)
[2] Bandyopadhyay S, Das B and Miller A E 1994 *Nanotechnology* **5** 113
[3] Keyes R W and Landauer R 1970 *IBM J. Res. Dev.* **14** 152
[4] Rugar D, Budakian R, Mamin H J and Chui B H 2004 *Nature* **430** 329
[5] Elzerman J M *et al* 2004 *Nature* **430** 431
[6] Xiao M, Martin I, Yablonovitch E and Jiang H W 2004 *Nature* **430** 435
[7] Molotkov S N and Nazin S S 1997 *Phys. Low-Dimens. Struct.* **10** 85
[8] Molotkov S N and Nazin S S 1995 *JETP Lett.* **62** 273
[9] Rafailov E U *et al* 2006 *Appl. Phys. Lett.* **88** 041101
Markus A *et al* 2003 *Appl. Phys. Lett.* **82** 1818
[10] Amasha S *et al* 2006 *Preprint* cond-mat/0607110
Amasha S *et al* 2007 *Preprint* 0707.1656
[11] Bakshi P, Broido D and Kempa K 1991 *J. Appl. Phys.* **70** 5150
[12] Bandyopadhyay S and Roychowdhury V P 1997 *Superlatt. Microstruct.* **22** 411
[13] Bandyopadhyay S 2005 *Superlatt. Microstruct.* **37** 77
[14] Anantram M and Roychowdhury V P 1999 *J. Appl. Phys.* **85** 1622
[15] Pramanik S *et al* 2007 *Nat. Nanotechnol.* **2** 216
[16] deSousa R and Das Sarma S 2003 *Phys. Rev.* B **67** 033301
[17] Knill E 2005 *Nature* **434** 39
[18] Salahuddin S and Datta S 2007 *Appl. Phys. Lett.* **90** 093503
[19] Cavin R K, Zhirnov V V, Hutchby J A and Bourianoff G I 2005 *Fluct. Noise Lett.* **5** C29
[20] Melnikov D V and Leburton J-P 2006 *Phys. Rev.* B **73** 155301
[21] Hirjibehedin C F, Lutz C P and Heinrich A J 2006 *Science* **312** 1021
[22] Zhang X W, Fan W J, Li S S and Xia J B 2007 *Appl. Phys. Lett.* **90** 193111
[23] Nembach H T *et al* 2005 *Appl. Phys. Lett.* **87** 142503
[24] Petta J R *et al* 2005 *Science* **309** 2180
[25] Koppens F H L *et al* 2006 *Nature* **442** 766
[26] Hanson R, Witkamp B, Vandersypen L M K, van Beveren L H W, Elzerman J M and Kouwenhoven L P 2003 *Phys. Rev. Lett.* **91** 196802
[27] *The International Technology Roadmap for Semiconductors* published by the Semiconductor Industry Association http://www.itrs.net